NANO LETTERS

2006
Vol. 6, No. 12
2804−2809

Polarization and Phase Control of Remote Surface-Plasmon-Mediated Two-Photon-Induced Emission and Waveguiding

Jess M. Gunn, Melinda Ewald, and Marcos Dantus*

Department of Chemistry, Michigan State University, East Lansing, Michigan 48824

Received August 15, 2006; Revised Manuscript Received September 27, 2006

ABSTRACT

We report here on the control of remote surface-plasmon-mediated two-photon-induced luminescence of dendritic silver nanoparticle aggregates as observed by femtosecond laser microscopy. With a focal spot diameter ~1 μm, polarized remote emission has been observed 99 μm from the focal spot. We show control over the regions of emission by changing the polarization of the incident beam and by changing the spectral phase of the laser pulse.

Metallic nanoparticles have been studied extensively in an effort to understand both their unique emissive properties, as seen throughout history in stained glass, and their more recently discovered ability to localize and enhance electromagnetic fields. In 1974, Fleischmann[1] reported that pyridine adsorbed on a roughened silver electrode produced a Raman spectrum 10^5-10^6 times greater than that which would be expected. This effect, now known as surface-enhanced Raman scattering (SERS), is due to nanoscale structures produced by roughening and their ability to localize surface plasmons[2,3] into "hot spots", or regions of amplified electromagnetic (EM) field, that make surface-enhanced spectroscopies,[4] including SERS, possible. The localization of surface plasmons has also been used to enhance multiphoton processes, as first reported in 1981.[5] This localized surface plasmon (LSP) resonance has led to a wide variety of applications.[6−11]

"Long-distance" propagation of surface plasmons, to distances tens of micrometers away from the excitation focus, can occur via surface plasmon waves (SPWs) and was first observed in finite structures in 2000.[12] Since then, work has been done to design waveguides[12−14] and develop structures that act as mirrors and beamsplitters for SPWs.[12,15] SPWs have also been used to mediate fluorescence resonance energy transfer over 120 nm by sandwiching a thin silver film between the donor and acceptor molecules.[16]

In dendritic nanoparticle structures, both local and long distance effects are possible because there are two types of surface plasmons: SPWs, which propagate along the metal surface, and LSPs, which are confined to individual metal nanoparticles.[17] The combination of these two types of surface plasmons allows EM radiation incident on a dendritic structure to propagate away from the focal spot along the surface (via SPWs) and then localize in a particular region (via LSPs), as illustrated in Figure 1. The SPWs are expected to be capable of traveling 100 μm in silver.[18]

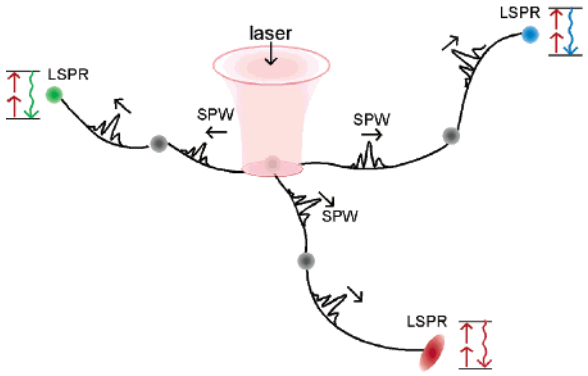

Figure 1. Cartoon representation of the observed remote surface-plasmon-mediated two-photon-induced luminescence of silver nanoparticle clusters. Energy from the laser at the focal spot travels via surface plasmon waves (SPWs) and induces localized surface plasmon resonance (LSPR) at discrete remote nanoparticles with distinct wavelength and polarization properties.

The difficulty in exploiting nanostructures that support both SPWs and LSPs is in controlling how the energy travels and where it localizes. Maier and Atwater[19] have laid out many of the considerations and possibilities for such guidance and localization. Additionally, Stockman and co-workers have carried out theoretical work in the field, proposing both

* Corresponding author: tel, 517-355-9715 ext 314; fax, 517-353-1793; e-mail, dantus@msu.edu.

10.1021/nl0619150 CCC: $33.50
Published on Web 10/31/2006

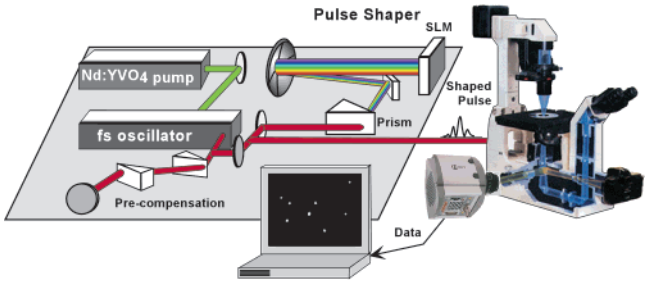

Figure 2. Setup for femtosecond laser scanning microscopy with pulse-shaping capabilities.

well-defined and random nanoscale structures that will permit coherent control of two-photon excitation to control plasmon localization with nanometer precision.[20,21] The experimental realization of such control would lead to advancements in what is perhaps the most exciting potential application of surface plasmons: surface-plasmon-based photonics (plasmonics). This rapidly growing field aims to bridge the gap between optics and electronics by carefully designing wires capable of carrying both electronic and optical signals over long distances.[22] In this paper, we present results demonstrating our ability to observe surface-plasmon-mediated two-photon-induced luminescence in a dendritic silver nanoparticle system up to 99 μm from the focal spot. We also show that we can control such luminescence by changing the polarization of the incident beam and by controlling the phase across the spectrum of the femtosecond laser pulse used for excitation. We attribute our ability to observe these phenomena to the combination of ultrashort pulses and a high (>90%) quantum efficiency imaging detector as described below.

The experimental setup is depicted in Figure 2. We used a titanium sapphire oscillator producing 12 fs pulses (bandwidth of 80 nm fwhm) centered near 800 nm, with a repetition rate of 97 MHz and 250 mW average power coupled with an inverted microscope via a short-pass (650 nm cutoff) dichroic mirror in the microscope. The sample rested on a piezoelectric nanopositioning stage which allowed the sample to be scanned over a range of 30 μm in the x and y directions. All experiments were carried out using a 60×/1.45 NA apochromatic objective with a focal spot size of ~0.5 μm, unless otherwise noted, to focus the beam onto the sample and collect the emitted light, which was then imaged by an electron multiplier CCD camera. Because of the dichroic mirror, laser scattered light (700−900 nm) is not detected. The multiphoton intrapulse interference phase scan (MIIPS) method[23−25] was used to eliminate high-order phase distortions to deliver transform-limited (zero-phase) pulses at the focus of the microscope objective. This allowed the introduction of calibrated phase functions to achieve coherent control over the two-photon-induced emission as presented in this paper.

The silver nanoparticles studied were synthesized by a citrate reduction,[26,27] and dendritic aggregate formation was induced by the addition of fumaric acid.[28] The aggregates precipitated onto quartz coverslips over 60 h, forming a thin film. The coverslips were then removed from the solution,

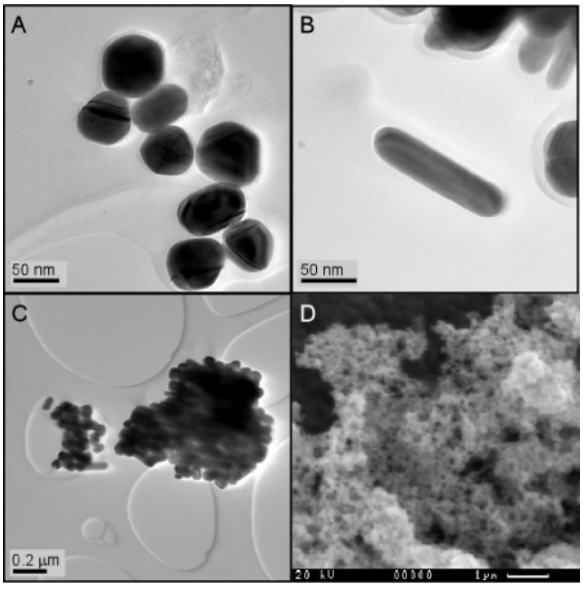

Figure 3. Panels A−C show TEM images of individual silver nanoparticles, which form both as roughly spherical structures and as rods. Panel D shows an SEM image of the structure of the aggregates formed.

rinsed in MilliQ water, and allowed to dry. Electron microscopy images were obtained in order to characterize the nanoparticle samples. Panels A−C of Figure 3 show transmission electron microscopy (TEM) images obtained of the samples, while panel D shows a scanning electron microscopy (SEM) image obtained. The TEM images indicate that the nanoparticles form both as roughly spherical structures (Figure 3A) and as rods (Figure 3B), with dimensions on the order of 50 nm, while the SEM image shows the dendritic nature of the nanoparticle aggregate film.

Average powers as low as 2 μW (~707 W/cm^2 average power; 7.28 × 10^9 W/cm^2 peak power) were found to cause irreversible damage to the sample in scanning experiments. In order to minimize laser damage and ensure the images were reproducible, the power of the incident laser beam was reduced below ~1 μW for scanning experiments. When collecting wide-field images, we found some regions that were stable under higher power excitation (95 μW). At these powers, we were able to image the remote emission from our sample and detect reproducible changes caused by altering the polarization or the spectral phase of the incident beam.

Excitation of the dendritic nanocluster films results in intense luminescence. The observed luminescence appears consistent with two-photon surface-plasmon-mediated luminescence of silver oxide on the surface of the silver nanoparticle films.[29−32] This is supported by a power study of dendritic silver nanoparticle aggregates in solution, in which a quadratic dependence of the signal on pulse intensity is observed, as shown in Figure 4. The spectra shown in Figure 4 are for dendritic silver nanoparticle aggregates prepared under air. Solutions prepared under N_2 have similar emission spectra (not shown) with slightly lower overall intensities.

Previous work in the group of Scherer has shown that localized second harmonic emission from silver nanoparticles

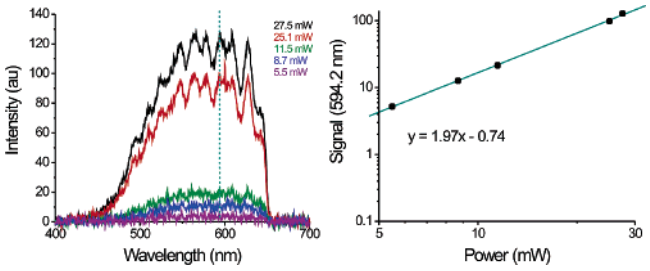

Figure 4. Two-photon-induced luminescence of dendritic silver nanoparticle aggregates in solution. The left panel shows the emission spectrum at different incident powers, while the right panel shows a plot of the emission intensity vs power on a log−log scale. The slope near 2 indicates the process is a two-photon process. The sharp cutoff at 650 nm in the left panel is due to the cutoff filter used to separate the incident beam from the emission.

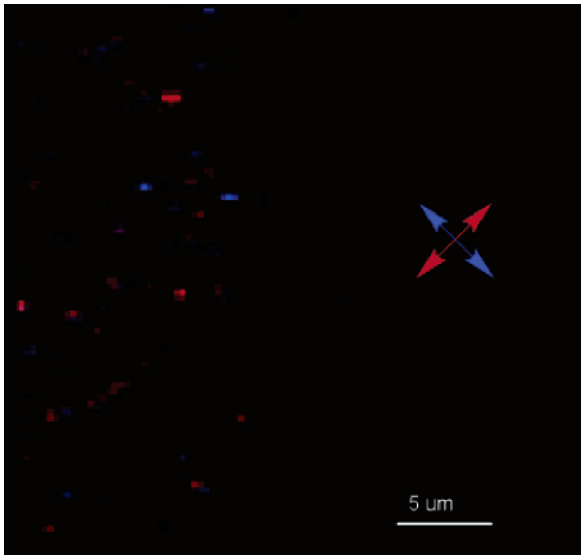

Figure 5. Control of local two-photon-induced fluorescence through alteration of the polarization of the incident laser beam. Areas that emitted when excited with a 45° polarized incident laser beam are false colored in red, whereas areas that emitted when excited with a 135° polarized incident laser beam are false colored in blue.

can be controlled by controlling the polarization of the excitation laser.[33] In Figure 5, we show a scanning experiment in which control of two-photon-induced fluorescence at the focal spot, via rotating the polarization of the excitation laser beam, is demonstrated.

When exciting the dendritic nanocluster films at a single point, relatively intense, highly localized emission can be observed tens of micrometers away when wide-field images are collected. This is illustrated in Figure 6, where the focal spot is located at (0,0), indicated by the crosshairs, and emission is observed as far as 99 μm from the focal spot. These data were obtained with a 40×/0.60 NA objective with a focal spot diameter of <1 μm. Note that some areas of remote emission are more intense than the emission observed at the focal spot. Significantly, we have observed remote emission not only from dendritic structures, as shown, but also from nanopatterned structures (results not shown) obtained from the Van Duyne group.

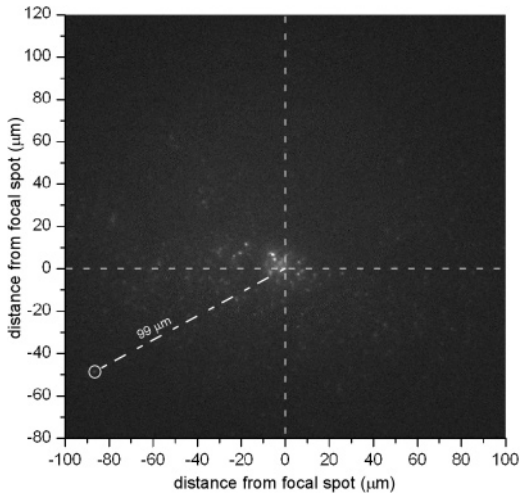

Figure 6. Remote emission. Two-photon-induced luminescence of the silver nanoparticles is observed at distances up to 99 μm from the focal spot (indicated by crosshairs).

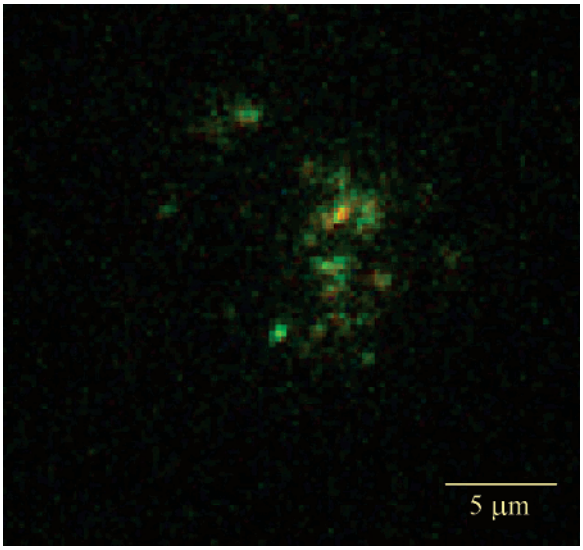

Figure 7. Composite image of remote emission collected with colored filters. Signal having wavelengths between 600 and 650 nm, wavelengths between 500 and 575 nm, and wavelengths less than 500 nm are false colored red, green, and blue, respectively.

The regions of emission detected far from the focal spot are not caused by laser scattering, because laser scattered light (700−900 nm) is rejected from the emission path by the 650 nm short-pass dichroic mirror in the setup. Additional tests using colored filters in the emission path were conducted and further confirm the absence of scattered light. When filters that block wavelengths greater than 700 nm were used, no change in emission intensity was observed. When a filter was added that transmits only wavelengths greater than 600 nm, weak emission was observed from a small number of locations (Figure 7, red). Most of the emission was observed when using a filter that transmits wavelengths between 500 and 575 nm (Figure 7, green), and only very weak emission was observed when a filter that transmits wavelengths less than 500 nm was used (Figure 7, blue, visible only as background noise). These results are consistent with the spectra of the dendritic nanoparticle aggregates in solution

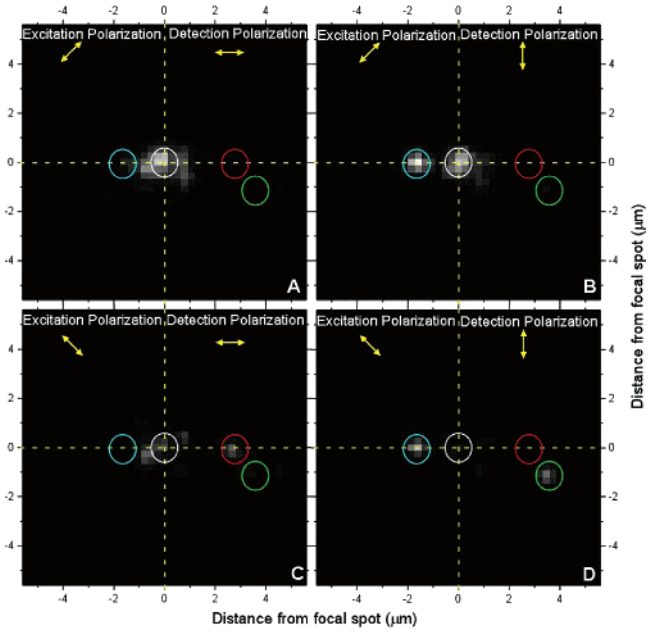

Figure 8. Polarization characteristics of dendritic silver thin films. Each panel is of the same area under different excitation and detection conditions. Panels A and B are excited with 45° polarized light, and panels C and D are excited with 135° polarized light. Horizontally polarized light was collected in panels A and C, and vertically polarized light was collected in panels B and D. This figure illustrates that the observed two-photon-induced luminescence is polarized, as the area in the blue ring shows, and that emission can be controlled by the incoming polarization, as shown by the area in the white ring.

(see Figure 4). Furthermore, in the spectral domain, the intensity would decay exponentially with wavelength. We see much more emission in the 500−575 nm spectral region than in the >600 nm region, as observed in the solution spectrum. Finally, if the observed remote emission was caused by scattered light, its intensity would decay as the square of the distance from the focus. Analysis of distance of remote emission versus intensity shows no correlation. From these observations we conclude that laser scatter is not consistent with the detected remote emission.

Figure 8 illustrates our work toward characterizing and controlling the polarization properties of remote emission. We observe that both the remote and local (at the focal spot) emissions are polarized and that the polarization of the incident beam is not always conserved, nor is the polarization of each region of emission the same. Each panel of Figure 8 is a wide-field image of the same area under different polarization conditions for excitation and emission. Panels A and B were excited with a beam of 45° polarized light, while panels C and D were excited with a beam of 135° polarized light. Horizontally polarized emission was detected in panels A and C, and vertically polarized emission was detected in panels B and D. It can be seen from this figure that the emission is polarized, with the spots not all having the same emission polarization. For example, the area in the blue ring emits distinctly vertically polarized light for both excitation polarizations, while the region ringed in red emits horizontally polarized light. Even emission from the region at the focal spot does not necessarily maintain the polarization of the excitation beam. Additionally, polarization of the excitation beam can be used to control the presence or absence of emission in certain spots. This is clearly illustrated by the focal spot, ringed in white, but has also been observed for remote emission, as shown by the red and green rings.

As a second control strategy, we have performed a series of measurements using shaped laser pulses. Our group has developed a number of strategies to control nonlinear optical excitation based on phase-shaped femtosecond laser pulses.[23,34−37] Here we explore the influence of phase-shaped pulses on the remote two-photon induced luminescence

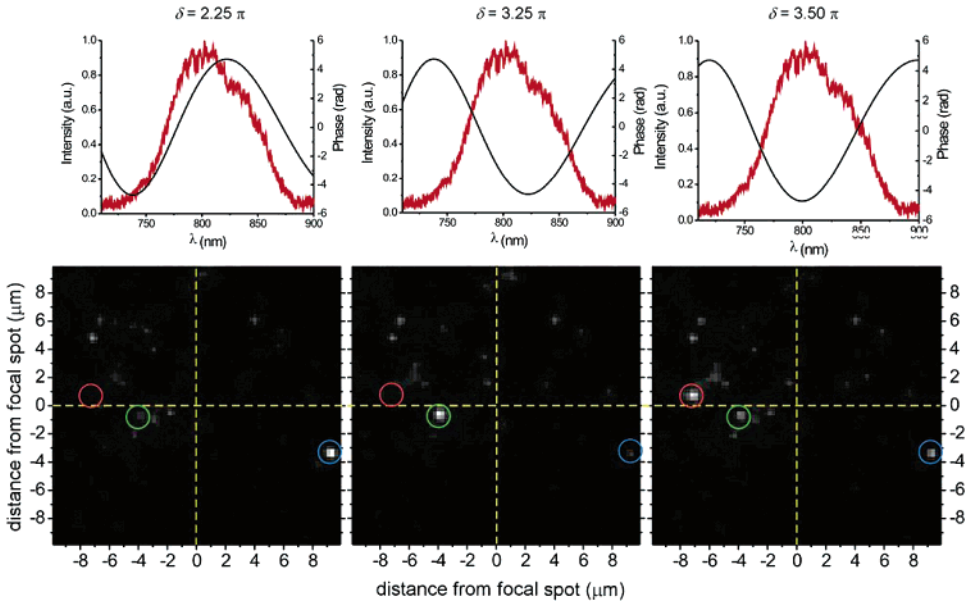

Figure 9. Phase control of remote emission. Each lower panel is a wide-field image of the same region of the sample, with the focal spot at (0, 0). The phases (black line) applied across the spectrum of the pulse (red line) are shown above each image. The colored circles highlight regions of interest and are at the same position in each panel.

exhibited by dendritic silver nanoparticle aggregates. Figure 9 shows three wide-field images of a region obtained using different sinusoidal phase functions of the form $1.5\pi \sin(12\omega - \delta)$ applied across the spectrum of the laser pulse, where the frequency, ω, is in fs^{-1}. In these images, only the value of δ (in rad) is varied from panel to panel. The use of fluorescent slides has confirmed that the focal spot does not move with the application of various phases. We find that some local hot spots are sensitive to the spectral phase of the excitation laser pulse. These images were repeated over two complete $\delta = 0-4\pi$ cycles to ensure reproducible dependence of emission on phase.

The presence of remote emission, and the ability to control it via polarization and phase, indicates that it is possible to control plasmonic waveguides and emission over macroscopic (tens of micrometers) distances. With a laser focused to a 1 μm^2 region, we were able to control localized emission over a 10^4 μm^2 area. This 4 orders-of-magnitude spatial control achieved with phase-shaped and polarized pulses, may have great significance in the field of electronics, in which miniaturization of chips is limited by the size of (and subsequent heat loss due to) the wires used to transport electronic information. The development of plasmonic waveguides will allow for controlled transport of optical information along nanowires, lowering the size barrier currently faced.

Acknowledgment. We gratefully acknowledge funding for this research from the Chemical Sciences, Geosciences and Biosciences Division, Office of Basic Energy Sciences, Office of Science, U.S. Department of Energy. We thank Professor Martin Crimp for the SEM and TEM images, and Dr. K. Willets and Professor Richard Van Duyne for providing nanopatterned samples. We also acknowledge an enlightening discussion with Professor Mark Stockman.

References

(1) Fleischmann, M.; Hendra, P. J.; McQuillan, A. J. Raman-Spectra of Pyridine Adsorbed at a Silver Electrode. *Chem. Phys. Lett.* **1974**, *26* (2), 163−166.
(2) Moskovits, M. Surface-Enhanced Spectroscopy. *Rev. Mod. Phys.* **1985**, *57* (3), 783−826.
(3) Link, S.; El-Sayed, M. A. Optical properties and ultrafast dynamics of metallic nanocrystals. *Annu. Rev. Phys. Chem.* **2003**, *54*, 331−366.
(4) Schatz, G. C.; Van Duyne, R. P. Electromagnetic Mechanism of Surface-Enhanced Spectroscopy. In *Handbook of Vibrational Spectroscopy*;; Chalmers, J. M., Griffiths, P. R., Eds.; Wiley: New York, 2002; pp 759−774.
(5) Heinz, T. F.; Chen, C. K.; Ricard, D.; Shen, Y. R., Optical 2nd-Harmonic Generation from a Monolayer of Centrosymmetric Molecules Adsorbed on Silver. *Chem. Phys. Lett.* **1981**, *83* (1), 180−182.
(6) Kneipp, K.; Wang, Y.; Kneipp, H.; Perelman, L. T.; Itzkan, I.; Dasari, R.; Feld, M. S. Single molecule detection using surface-enhanced Raman scattering (SERS). *Phys. Rev. Lett.* **1997**, *78* (9), 1667−1670.
(7) Nie, S. M.; Emery, S. R. Probing single molecules and single nanoparticles by surface-enhanced Raman scattering. *Science* **1997**, *275* (5303), 1102−1106.
(8) Kim, W.; Safonov, V. P.; Shalaev, V. M.; Armstrong, R. L. Fractals in microcavities: Giant coupled, multiplicative enhancement of optical responses. *Phys. Rev. Lett.* **1999**, *82* (24), 4811−4814.
(9) Kelly, K. L.; Coronado, E.; Zhao, L. L.; Schatz, G. C. The optical properties of metal nanoparticles: The influence of size, shape, and dielectric environment. *J. Phys. Chem. B* **2003**, *107* (3), 668−677.
(10) McFarland, A. D.; Van Duyne, R. P. Single silver nanoparticles as real-time optical sensors with zeptomole sensitivity. *Nano Lett.* **2003**, *3* (8), 1057−1062.
(11) Lee, S. J.; Morrill, A. R.; Moskovits, M. Hot spots in silver nanowire bundles for surface-enhanced Raman spectroscopy. *J. Am. Chem. Soc.* **2006**, *128* (7), 2200−2201.
(12) Charbonneau, R.; Berini, P.; Berolo, E.; Lisicka-Shrzek, E. Experimental observation of plasmon-polariton waves supported by a thin metal film of finite width. *Opt. Lett.* **2000**, *25* (11), 844−846.
(13) Stockman, M. I. Nanofocusing of optical energy in tapered plasmonic waveguides. *Phys. Rev. Lett.* **2004**, *93*, 137404.
(14) Dionne, J. A.; Sweatlock, L. A.; Atwater, H. A.; Polman, A. Planar metal plasmon waveguides: frequency-dependent dispersion, propagation, localization, and loss beyond the free electron model. *Phys. Rev. B* **2005,** *72*, 075405.
(15) Ditlbacher, H.; Krenn, J. R.; Schider, G.; Leitner, A.; Aussenegg, F. R., Two-dimensional optics with surface plasmon polaritons. *Appl. Phys. Lett.* **2002**, *81* (10), 1762−1764.
(16) Andrew, P.; Barnes, W. L. Energy transfer across a metal film mediated by surface plasmon polaritons. *Science* **2004**, *306* (5698), 1002−1005.
(17) Shalaev, V. M.; Botet, R.; Mercer, J.; Stechel, E. B. Optical properties of self-affine thin films. *Phys. Rev. B* **1996**, *54* (11), 8235−8242.
(18) Barnes, W. L.; Dereux, A.; Ebbesen, T. W. Surface plasmon subwavelength optics. *Nature* **2003**, *424* (6950), 824−830.
(19) Maier, S. A.; Atwater, H. A. Plasmonics: Localization and guiding of electromagnetic energy in metal/dielectric structures. *J. Appl. Phys.* **2005**, *98*, 011101.
(20) Stockman, M. I.; Faleev, S. V.; Bergman, D. J., Coherent control of femtosecond energy localization in nanosystems. *Phys. Rev. Lett.* **2002,** *88*, 067402.
(21) Stockman, M. I.; Hewageegana, P. Nanolocalized nonlinear electron photoemission under coherent control. *Nano Lett.* **2005**, *5* (11), 2325−2329.
(22) Ozbay, E. Plasmonics: Merging photonics and electronics at nanoscale dimensions. *Science* **2006,** *311* (5758), 189−193.
(23) Dela Cruz, J. M.; Pastirk, I.; Lozovoy, V. V.; Walowicz, K. A.; Dantus, M. Multiphoton intrapulse interference 3: Probing microscopic chemical environments. *J. Phys. Chem. A* **2004**, *108* (1), 53−58.
(24) Lozovoy, V. V.; Pastirk, I.; Dantus, M. Multiphoton intrapulse interference. IV. Ultrashort laser pulse spectral phase characterization and compensation. *Opt. Lett.* **2004**, *29* (7), 775−777.
(25) Xu, B.; Gunn, J. M.; Dela Cruz, J. M.; Lozovoy, V. V.; Dantus, M. Quantitative investigation of the multiphoton intrapulse interference phase scan method for simultaneous phase measurement and compensation of femtosecond laser pulses. *J. Opt. Soc. Am. B* **2006**, *23* (*Doc. ID 61987*), 750−759.
(26) Turkevich, J.; Stevenson, P. C.; Hillier, J. A Study of the Nucleation and Growth Processes in the Synthesis of Colloidal Gold. *Discuss. Faraday Soc.* **1951** (*11*), 55−74.
(27) Lee, P. C.; Meisel, D. Adsorption and Surface-Enhanced Raman of Dyes on Silver and Gold Sols. *J. Phys. Chem.* **1982**, *86* (17), 3391−3395.
(28) Butenko, A. V.; Shalaev, V. M.; Stockman, M. I., Fractals—Giant Impurity Nonlinearities in Optics of Fractal Clusters. *Z. Phys. D*: *Atoms, Mol. Clusters* **1988**, *10* (1), 81−92.
(29) Peyser, L. A.; Lee, T. H.; Dickson, R. M. Mechanism of Ag-n nanocluster photoproduction from silver oxide films. *J. Phys. Chem. B* **2002**, *106* (32), 7725−7728.
(30) Gleitsmann, T.; Stegemann, B.; Bernhardt, T. M. Femtosecond-laser-activated fluorescence from silver oxide nanoparticles. *Appl. Phys. Lett.* **2004**, *84* (20), 4050−4052.
(31) Lehmann, J.; Merschdorf, M.; Pfeiffer, W.; Thon, A.; Voll, S.; Gerber, G. Surface plasmon dynamics in silver nanoparticles studied by femtosecond time-resolved photoemission. *Phys. Rev. Lett.* **2000,** *85* (14), 2921−2924.
(32) Kubo, A.; Onda, K.; Petek, H.; Sun, Z. J.; Jung, Y. S.; Kim, H. K. Femtosecond imaging of surface plasmon dynamics in a nanostructured silver film. *Nano Lett.* **2005**, *5* (6), 1123−1127.
(33) Jin, R. C.; Jureller, J. E.; Kim, H. Y.; Scherer, N. F. Correlating second harmonic optical responses of single Ag nanoparticles with morphology. *J. Am. Chem. Soc.* **2005**, *127* (36), 12482−12483.

(34) Walowicz, K. A.; Pastirk, I.; Lozovoy, V. V.; Dantus, M. Multiphoton intrapulse interference. 1. Control of multiphoton processes in condensed phases. *J. Phys. Chem. A* **2002**, *106* (41), 9369−9373.
(35) Lozovoy, V. V.; Pastirk, I.; Walowicz, K. A.; Dantus, M. Multiphoton intrapulse interference. II. Control of two- and three-photon laser induced fluorescence with shaped pulses. *J. Chem. Phys.* **2003**, *118* (7), 3187−3196.
(36) Comstock, M.; Lozovoy, V. V.; Pastirk, I.; Dantus, M. Multiphoton intrapulse interference 6; binary phase shaping. *Opt. Express* **2004**, *12* (6), 1061−1066.
(37) Lozovoy, V. V.; Dantus, M. Coherent control in femtochemistry. *ChemPhysChem* **2005**, *6* (10), 1970−2000.

NL0619150